

Large-scale surface reconstruction energetics of Pt(100) and Au(100) by all-electron DFT

Paula Havu^{1,*}, Volker Blum¹, Ville Havu^{1,2}, Patrick Rinke¹, and Matthias Scheffler¹

1) *Fritz-Haber-Institut, Berlin, Germany* and

2) *Department of Applied Physics, Aalto University, Helsinki, Finland*

(Dated: March 13, 2019)

The large-scale quasihexagonal surface reconstructions of Au(100) and Pt(100) are among the biggest surprises of early surface science. Still, some significant questions regarding their reconstruction energies remain even today (rather dissimilar Au and Pt in the available experiments, and experiment and theory do not match for Pt). We here use density-functional theory in an all-electron implementation and large enough approximant supercells—“(5×N)”, $N=10-30$ —to show that the reconstruction energies of both surfaces are in fact similar, and closer to the measured value for Pt(100) *in vacuo*. Additionally, our calculations demonstrate excellent agreement with known geometry characteristics of both surfaces and corroborate earlier work that suggested relativistically enhanced *d-d* hybridization as the driving force of the reconstruction.

PACS numbers: 68.35.B-, 68.35.Md, 71.15.Mb, 73.20.At

Compared to most other metals, the late 5*d* transition metals Pt and Au (and also Ir) are special in that their low-index surfaces (100), (110) and (111) *reconstruct* for a range of thermal or environmental conditions.[1–6] This peculiarity has been a source of continued interest since the early days of surface science up to the present,[7] but also has considerable practical implications: The surface structural equilibria of Pt and Au can not be neglected whenever one seeks to understand the mechanisms that govern their applications in, e.g., catalysis, electrochemistry, electronics or even jewelry (corrosion resistance). However, developing a fully quantitative picture faces a significant obstacle at least for the (100) surfaces, due to the sheer size of their reconstructed unit cells. The (100) surface plane abandons the square arrangement of the fcc bulk entirely, forming instead an almost perfectly *hexagonal* (“hex”) layer, [8–21] whose atomic rows are slightly rotated (0.5–1°) against the underlying (100) surface rows.[10, 11, 14, 18, 19] Per unit area, this plane contains approximately 25 % *more* atoms than a primitive (100) plane. The lateral variations of the atomic positions in the “hex” layer give rise to a considerable local buckling, which has been observed qualitatively by STM[13, 20, 21] and empirical potential calculations,[21] but has not been quantified to date by diffraction experiments or by first-principles approaches. In fact, the superstructure is, strictly, incommensurate[13–16, 18, 19, 21] both for Au and for Pt. This would not be a grave obstacle for either current experiments or theory *if* suitably accurate, small periodic approximants for the full surface structure could be found. However, it turns out that the smallest approximants which cover all the features mentioned above (2-dimensional lateral contraction and slight rotation) are already significant in size themselves: Roughly speaking, “(5×N)”,[2, 8, 10, 11] where $N \approx 20-30$, i.e., ≥ 100 atoms to be considered in each layer.

The goal of the present paper is a quantitative assess-

ment of the surface properties of Au(100) and Pt(100) with sufficiently large “(5×N)” approximants, from first principles and with full all-electron accuracy. Although challenging, we show that such simulations are now feasible. We demonstrate that large “(5×N)” unit cells are not only necessary to assess the local surface structure, but also allow to clear up some apparent contradictions regarding the reconstruction energy which arise from using smaller unit cells or (experimentally) a non-vacuum surface environment.

Concerning the reconstruction energy and driving force, some significant *qualitative* lessons can already be learned from simple (1×1) surface models. Using density functional theory (DFT) in the local-density approximation (LDA), Takeuchi, Chan, and Ho (TCH) [22] demonstrated that free-standing Au(111) planes enjoy a large energy gain when uniformly contracted to the interatomic spacing of the Au(100) “hex” reconstruction. Using a Frenkel-Kontorova model, TCH found a net surface energy gain through reconstruction, albeit very small: $\Delta E_{\text{hex}} < 0.01$ eV per unit area of the (100) surface [eV/1×1]. This is not far from an experimental, electrochemical estimate (0.02 eV/1×1 [23]), but, puzzlingly, smaller by a factor ≈ 6 than a careful assessment of the reconstruction energy of Pt(100) *in vacuo*, 0.12 eV/1×1 [24] (an earlier analysis placed Pt(100) even higher, at 0.21 eV/1×1 [25, 26]). Adding to the confusion is the fact that theoretical estimates for Pt(100) based on small (5×1) approximant cells *in vacuo* yield only half the experimental value (0.05–0.07 eV/1×1 [27–29]). For Au(100), (5×1)-based theoretical estimates[30–32] are approximately in line with the electrochemical experiments. Since Au(100) and Pt(100) do behave similarly also regarding thermal stability,[18, 19] one might consider the experimental reconstruction energy estimate for Pt(100) an outlier—if it were not for the fact that it is *this* experiment which pertains to the full reconstruction

in the vacuum environment, and not to an electrochemical environment, or to a restricted unit cell.

Remarkably, our calculations of the full $(5 \times N)$ reconstruction energy resolve this puzzle in favor of the Pt(100) experiment, and show that both the experimental and theoretical values for Au(100) above underestimate the reconstruction energy. In addition, we demonstrate perfect structural agreement between our simulations and those elements of the structure which are experimentally known. Finally, we have access to the full surface electronic structure, allowing us to support relativistically enhanced d - d hybridization as the driving force for the reconstruction, as surmised by TCH [22].

Figure 1 shows the unit cells of the specific approximants that are important for this work. In each case, the hexagonal top layer (circles) is slightly distorted to form a commensurate coincidence lattice (arrows) with the underlying square substrate (crosses). Subfigure (a) shows the popular (5×1) approximant. Compared to an ideal hexagonal layer, the top layer is compressed by 4 % in one dimension but not in the other. To account for the reconstruction in both dimensions, larger $(5 \times N)$ -type approximants ($N \approx 20-30$) are needed. In subfigure (b), the hexagonal plane is thus compressed in *both* dimensions, and somewhat distorted so that its close-packed rows are additionally rotated by $\approx 1^\circ$ against the substrate. Finally, subfigure (c) shows a closely related $(5 \times N)$ -type approximant, with a rotation of $\approx 1^\circ$ in both dimensions.[10, 11, 13–15, 18, 21] We model the “hex” layers as part of five-layer slabs (two layers relaxed, three kept fixed in bulk positions) that are separated by more than 25 Å of vacuum. The largest slabs thus comprise 786 atoms, 336 of which are fully relaxed. Our work is enabled by our efficient, scalable, and accurate all-electron “DFT and beyond” code FHI-aims [33, 34] on IBM’s massively parallel BlueGene/P.

Compared to a (1×1) layer, a $(5 \times N)$ plane ($N > 1$) contains $(N+5+1)$ additional atoms in the unit cell. In terms of total energies for individual surface slabs, E^{slab} , and the total energy per atom in the bulk, $E^{\text{atom,bulk}}$, the reconstruction energy $\Delta E_{5 \times N}$ (here defined to be positive if a reconstruction is favored) is

$$-\Delta E_{5 \times N} = E_{5 \times N}^{\text{slab}} - 5N E_{1 \times 1}^{\text{slab}} - (N+6) E^{\text{atom,bulk}}. \quad (1)$$

All DFT total energies are based on the LDA,[35] or the generalized gradient functional PBE.[36] We use fcc lattice parameters $a_{\text{Au}}=4.055$ (4.169) Å and $a_{\text{Pt}}=3.899$ (3.974) Å in LDA (PBE), respectively, computed for the highly converged *tier 1* basis level (*spdfg* for Pt, *spdfgh* for Au [33]), and essentially converged already for $(10 \times 10 \times 10)$ k -point grids. The *tier 1* basis set level is also used to obtain converged geometry relaxation (residual forces $< 10^{-2}$ eV/Å) and total energies for all surfaces considered here. The convergence of our surface calculations is verified by explicit tests for (5×1) approximants

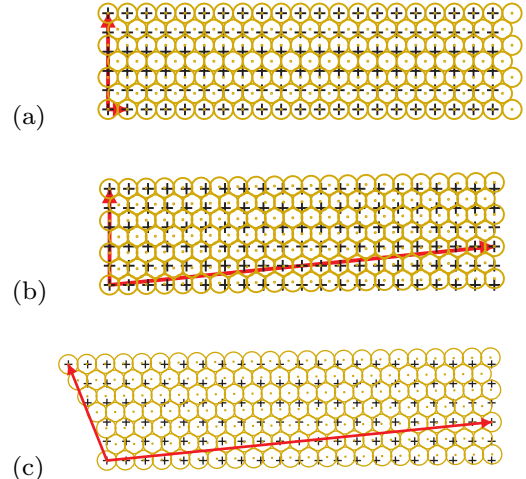


FIG. 1: Structure and distortion of the quasihexagonal layer. Circles: topmost (“hex”) layer, crosses: second (square) layer. Unit vectors of the coincidence lattice of both planes are shown in red. (a) (5×1) and (b) (5×20) superstructure. The “hex” layer is compressed by 4% wrt. bulk (111) in both dimensions, and rotated by 1° in one dimension. (c) (5×20) -like superstructure, rotated in both dimensions.

(a-c below): (a) Compared to (much larger) *tier 2* basis sets, reconstruction energies are converged to better than 0.003 eV/ 1×1 . (b) Nine-layer slabs (four relaxed) yield an energy lowering of 0.01 eV/ 1×1 for Au and Pt. (c) 0.01 eV/ 1×1 accuracy is obtained by 10×10 k -point grids in units equivalent to the 1×1 cell. In our calculations with variable cell length N , we further reduce the k -grid noise by using 2×2 and equivalent k -grids below $N=20$, and 1×2 and equivalent k -meshes for $N \geq 20$. In terms of the 1×1 periodicity, this amounts to 20×1 or denser grids throughout this work. Our *overall* accuracy is verified by explicit FP-LAPW [37] (5×1) calculations, yielding agreement within 0.01 eV/ 1×1 .

Figure 2 summarizes our results regarding $\Delta E_{5 \times N}$ for Pt(100) and Au(100), using the approximant cells Fig. 1a and b. Since the density of $(5 \times N)$ planes increases as N decreases, we plot $\Delta E_{5 \times N}$ as a function of the *lateral atomic packing density* relative to the underlying (100) lattice: $\theta = n_{\text{hex}}/n_{100}$. Experimentally, SXRD yields $\theta \approx 1.242-1.250$ for Pt(100)[18, 19] and 1.259 for Au(100).[15, 18] We find that the *two-dimensional* $(5 \times N)$ compression is indeed energetically favored over (5×1) both in LDA and PBE. In essence, the energy surface shows shallow minima that are precisely in line with the experimental analysis. The experimental trend of a denser “hex” layer for Au than for Pt is clearly confirmed. For Pt, the energy gain of $(5 \times N)$ over (5×1) is small (~ 0.01 eV/ 1×1), but Au roughly *doubles* its reconstruction energy. This change brings the reconstruction energies of both surfaces close to one another, and

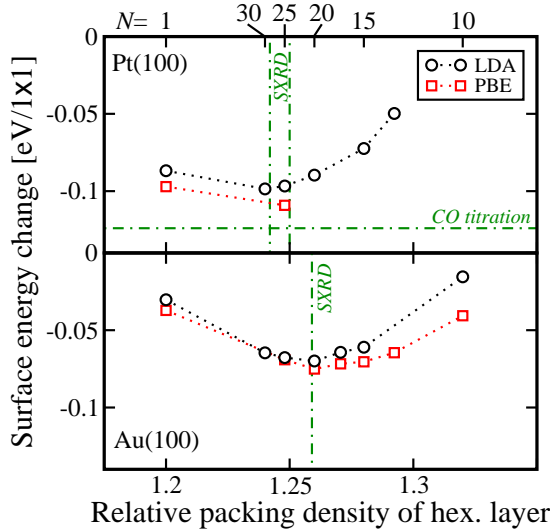


FIG. 2: Change of surface energy with reconstruction, compared to (1×1) [negative of $\Delta E_{5 \times N}$, Eq. (1)], for Pt(100) (upper panel) and Au(100) (lower panel) using DFT-LDA/PBE, as a function of the lateral atomic packing density θ . Dash-dotted lines: Experimental estimates for the packing density from SXRD,[18, 19] and for the Pt(100) reconstruction energy from the reanalysis [24] of CO titration calorimetry data.[25, 26]

also to the experimental reconstruction energy estimate for Pt(100). In numbers, we find $\Delta E_{5 \times N} = 0.07$ eV/ 1×1 (Au) vs. 0.10 eV/ 1×1 (Pt) in DFT-LDA. In PBE, the reconstructed surface energies are even slightly lower: for Pt, $\Delta E_{5 \times N} = 0.11$ eV/ 1×1 (PBE) is in remarkably close agreement with experiment (0.12 ± 0.02 eV/ 1×1 [24]), and we recall that we even expect a further lowering by ≈ 0.01 eV/ 1×1 for the theoretical value from relaxation beyond the second layer, as indicated by (5×1) approximants with thicker slabs (see above). We thus conclude that *there is no contradiction*[27–29, 38] between theory and experiment for Pt(100), and that the reconstruction energies of Au(100) and Pt(100) are similar when the same in *vacuo* conditions are applied. In our view, the seeming agreement for Au(100)- (5×1) theory in *vacuo* and electrochemical experiments was accidental.

As a final check, we computed the energy difference between the partially and fully rotated approximants in Figs. 1b and c for Au(100) in LDA at the optimum packing density (5×20). The energy gain amounts to 4 meV/ 1×1 in favor of the approximant closest to experiment, Fig. 1c. [Between a competely unrotated (5×20) cell and the uniformly rotated cell of Fig. 1c, the change would be 8 meV/ 1×1 .] We note that this gain is small but significant when taken per reconstructed unit cell, and underscores the level of precision reached by our first-principles treatment.

Figure 3 shows a top view (“hex” layer only) of the (5×20) reconstructed Au(100) surface in LDA. Qual-

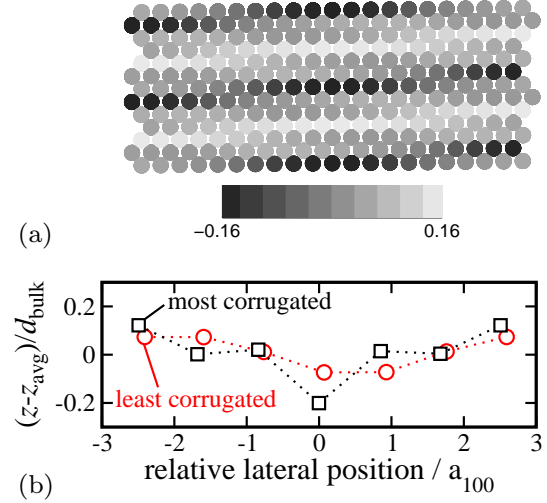


FIG. 3: (a) Top view of the “hex” layer on an Au(100)- (5×20) reconstruction model (LDA). z coordinates of all atoms are color-coded in units of d_{bulk} , relative to the average z position of the plane. (b) Height profiles through the most corrugated and least corrugated surface areas.

itatively, this picture looks strikingly similar to published atomically resolved STM images.[20, 21] For a more quantitative view, the frame below shows the z coordinate of atomic zigzag rows in the “5” direction with the largest and smallest corrugation amplitude, respectively. The variation illustrates strikingly that very different local environments exist in the surface as a result of the *two-dimensional* reconstruction. The maximum corrugation in the “5” direction is 0.65 Å (32% of the bulk interlayer spacing d_{bulk}), compared to only 15% in the least corrugated area. These numbers are very similar in LDA and PBE, and also very similar to Pt(100)- (5×25) (29% and 14%, respectively).

Table I compares some key surface geometry parameters from our study with the available diffraction experiments. The agreement is remarkable, especially since the most detailed study [17] used a surface-averaged (5×1) model for Au(100), yielding a “hex” layer buckling in between our maximum and minimum corrugations.

Finally, we turn briefly to the electronic-structure changes that accompany the reconstruction. For 5d metals, relativity enhances the participation of the valence d electrons by shifting them upwards towards the s levels.[40, 41] Since d electrons are thus more easily promoted to sp -like states, enhanced sp bonding has been proposed as a cause of the reconstruction.[9, 42] On the other hand, enhanced bonding among the d states themselves was favored in Ref. [22]. Fig. 4 shows the energies of the valence band centers of the surface layer projected densities of states of Ir(100), Pt(100), and Au(100) (all three reconstruct) and Au(100) without relativity, or Ag(100) (the latter two surfaces would not reconstruct).

Au(100)		Pt(100)	
This work	Experiment	This work	Experiment
b_1/d_{bulk}	0.32(0.32)	0.275 ^a	0.29(0.29) $\approx 0.2^b$
			0.25-0.38 ^c
b_2/d_{bulk}	0.044(0.044)	0.069 ^a	0.042(0.042)
d_{12}/d_{bulk}	1.21(1.22)	1.20 ^a	1.20(1.20)
d_{23}/d_{bulk}	0.99(0.98)	0.99(1.00)	

TABLE I: Averaged interlayer distances d_{ij} and peak-to-peak buckling amplitudes b_i for Au(100)-(5×20) and Pt(100)-(5×25) in LDA (PBE in brackets), compared to experiment: ^aSXRD, Refs. [17]; ^bLEED, Ref. [12]; ^cHelium atom scattering, Ref. [39].

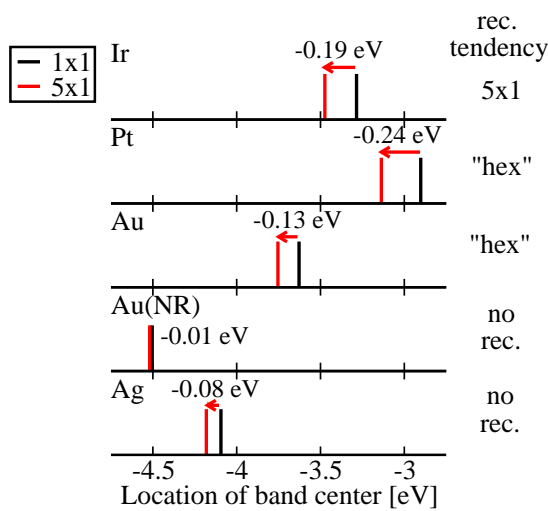


FIG. 4: Location of valence band centers of the projected densities of states (LDA) of the surface atoms of 5d(100)-(1×1) (black sticks) vs. (5×1) (red sticks) “hex” approximants, for various elements. Au(NR) denotes Au, but with a non-relativistic kinetic energy. The actual reconstruction tendency of each element is given in the right column.

In each case, vertical bars indicate the location for (1×1) (black) and (5×1) (red). In short, a characteristic downward shift of the valence band center accompanies the change for surfaces that reconstruct, whereas this shift is much smaller for the two surfaces that do not reconstruct. At the same time, an angular momentum decomposition of the changes shows only a tiny transfer of electrons between the d and sp channels, so the associated change must happen within the d states themselves. Taken together, this analysis thus supports the relativistically enhanced d - d hybridization mechanism suggested by TCH [22].

- [1] S. Hagstrom, H. B. Lyon, and G. A. Somorjai, Phys. Rev. Lett. **15**, 491 (1965).
- [2] D. G. Fedak and N. A. Gjostein, Phys. Rev. Lett. **16**, 171 (1966); Acta Met. **15**, 827 (1967); Surf. Sci. **8**, 77 (1967).
- [3] G. A. Somorjai, Surf. Sci. **8**, 98 (1967).
- [4] H. P. Bonzel and R. Ku, J. Vac. Sci. Tech. **9**, 663 (1972).
- [5] J. Perdereau, J. P. Biberian, and G. E. Rhead, J. Phys. F **4**, 798 (1974).
- [6] A. R. Sandy *et al.*, Phys. Rev. Lett. **68**, 2192 (1992).
- [7] M. S. Pierce *et al.*, Phys. Rev. Lett. **103**, 165501 (2009).
- [8] P. W. Palmberg and T. N. Rhodin, Phys. Rev. **161**, 586 (1967).
- [9] T. N. Rhodin, P. W. Palmberg, and E. W. Plummer, in *The structure and chemistry of solid surfaces*, edited by G. A. Somorjai (1969), pp. 22–1.
- [10] P. W. Palmberg, in *The structure and chemistry of solid surfaces*, edited by G. A. Somorjai (1969), pp. 29–1.
- [11] P. Heilmann, K. Heinz, and K. Müller, Surf. Sci. **83**, 487 (1979).
- [12] M. A. van Hove *et al.*, Surf. Sci. **103**, 218 (1981).
- [13] G. Binnig *et al.*, Surf. Sci. **144**, 321 (1984).
- [14] K. Yamazaki *et al.*, Surf. Sci. **199**, 595 (1988).
- [15] D. Gibbs *et al.*, Phys. Rev. B **42**, 7330 (1990).
- [16] D. Gibbs *et al.*, Phys. Rev. Lett. **67**, 3117 (1991).
- [17] B. M. Ocko *et al.*, Phys. Rev. B **44**, 6429 (1991).
- [18] D. L. Abernathy *et al.*, Phys. Rev. B **45**, 9272 (1992).
- [19] D. L. Abernathy *et al.*, Surf. Sci. **283**, 260 (1993).
- [20] A. Borg, A. M. Hilmen, and E. Bergene, Surf. Sci. **306**, 10 (1994).
- [21] G. Ritz *et al.*, Phys. Rev. B. **56**, 10518 (1997).
- [22] N. Takeuchi, C. T. Chan, and K. M. Ho, Phys. Rev. B **43**, 14363 (1991).
- [23] E. Santos and W. Schmickler, Chem. Phys. Lett. **400**, 26 (2004).
- [24] W. A. Brown, R. Kose, and D. A. King, Chem. Rev. **98**, 797 (1998).
- [25] Y. Y. Yeo, C. E. Wartnaby, and D. A. King, Science **268**, 1731 (1995).
- [26] Y. Y. Yeo, L. Vattoume, and D. A. King, J. Chem. Phys. **104**, 3810 (1996).
- [27] C. S. Chang *et al.*, Phys. Rev. Lett. **83**, 2604 (1999).
- [28] P. van Beurden and G. J. Kramer, J. Chem. Phys. **121**, 2317 (2004).
- [29] N. A. Deskins, J. Lauterbach, and K. T. Thomson, J. Chem. Phys. **122**, 184709 (2005).
- [30] Y. J. Feng, K. P. Bohnen, and C. T. Chan, Phys. Rev. B **72**, 125401 (2005).
- [31] T. Jacob, Electrochimica Acta **52**, 2229 (2007).
- [32] S. Venkatachalam *et al.*, Chem. Phys. Lett. **455**, 47 (2008).
- [33] V. Blum *et al.*, Comp. Phys. Comm. **180**, 2175 (2009).
- [34] V. Havu *et al.*, J. Comp. Phys. **228**, 8367 (2009).
- [35] J. Perdew and Y. Wang, Phys. Rev. B **45**, 13244 (1992).
- [36] J. Perdew, K. Burke, and M. Ernzerhof, Phys. Rev. Lett. **77**, 3865 (1996).
- [37] P. Blaha *et al.*, *Wien2k, an Augmented Plane Wave Plus Local Orbitals Program for Calculating Crystal Properties, Ed. Wien2k_03* (TU Wien, 2003).
- [38] P. Ghosh *et al.*, J. Chem. Phys. **126**, 244701 (2007).
- [39] X.-C. Guo *et al.*, Surf. Sci. **278**, 263 (1992).
- [40] J. P. Desclaux and P. Pyykkö, Chem. Phys. Lett. **39**, 300 (1976).
- [41] P. Pyykkö, Angew. Chem. Int. Ed. **43**, 4412 (2004).

* Present address: Helsinki University of Technology (TKK), Finland

[42] J. F. Annett and J. E. Inglesfield, *J. Phys.: Condens. Matter* **1**, 3645 (1989).